International Journal of Applied Pharmaceutics

ISSN- 0975-7058 Vol 18, Issue 2, 2026

Original Article

DESIGN, PHYSICOCHEMICAL CHARACTERIZATION, AND DEVELOPMENT OF A MATRIX DIFFUSION-CONTROLLED TRANSDERMAL PATCH OF RASAGILLINE FOR SUSTAINED ANTI-PARKINSON'S THERAPY

AHMED A. MOHAMED[1], MOHAMED A. ABDEL SALAM[2], DALIA A. GABER[2,3*], EMAN AL-JOHANI[3], SIHAM ABDOUN[4]

[1]Department of Pharmacology, College of Pharmacy, Al-Ahram Canadian University, Giza Governorate-3222401, Egypt. [2]Department of Pharmaceutics, College of Pharmacy, Al-Ahram Canadian University, Giza Governorate-3222401, Egypt. [3]Clinical Pharmacy Program, College of Health Sciences, Al-Rayan National College, Madina, Saudi Arabia. [4]Department of Pharmaceutics, College of Pharmacy, Qassim University, Qassim-51452, Saudi Arabia

[*]Corresponding author: Ahmed A. Mohamed; [*]Email: d.gaber1900@gmail.com

Received: 11 Sep 2025, Revised and Accepted: 08 Jan 2026

ABSTRACT

Objective: This study aimed to design and evaluate diffusion-controlled transdermal patches of rasagiline for sustained management of Parkinson's disease.

Methods: Matrix patches were prepared using the selected copolymers with 30% w/w dibutyl phthalate as plasticizer. Patches were evaluated for mechanical, physicochemical, and permeability characteristics. Drug–polymer compatibility was confirmed by Fourier Transform Infrared Spectroscopy (FTIR) and Differential Scanning Calorimetry (DSC). Various permeation enhancers (isopropyl myristate [IPM], eucalyptus oil, Span® 80, Tween® 20, and limonene) were incorporated at 2–10% w/w, and their effects were assessed through *in vitro* and ex vivo studies using Franz diffusion cells.

Results: All rasagiline patches exhibited smooth surfaces, flexibility, and uniform thickness. FTIR and DSC confirmed absence of drug–excipient interactions. The optimized RL: RS (7:3) formulation achieved a sustained 92.3% cumulative drug release after 24 h, following Higuchi diffusion kinetics. Among all enhancers, IPM (10% w/w) produced the highest improvement, yielding a 5.4-fold increase in skin flux (53.7 µg/cm^2·h) compared to control, and a total permeation of 1,342.9 µg/cm^2 after 24 h.

Conclusion: The optimized rasagiline patch composed of Eudragit® RL: RS (7:3) and 10% IPM achieved controlled drug release and significantly enhanced transdermal permeation. This system demonstrates strong potential for improving rasagiline bioavailability and patient compliance in Parkinson's disease therapy.

Keywords: Rasagiline, Transdermal patch, Diffusion control, Permeation enhancer, Parkinson's disease

DOI: https://dx.doi.org/10.22159/ijap.2026v18i2.56843 Journal homepage: https://innovareacademics.in/journals/index.php/ijap

INTRODUCTION

Parkinson's disease (PD) is a chronic, progressive neurodegenerative disorder characterized by the degeneration of dopaminergic neurons in the substantia nigra pars compacta, resulting in striatal dopamine deficiency. Clinically, PD presents with hallmark motor symptoms such as bradykinesia, rigidity, tremors, and postural instability, along with several non-motor manifestations including sleep disturbances, cognitive impairment, and autonomic dysfunction [1, 2]. The global burden of PD has been steadily increasing, and epidemiological studies project that its prevalence will nearly double by 2030 due to the aging population and lifestyle-related risk factors [3]. This rapid increase highlights the urgent demand for novel therapeutic approaches that can provide more consistent disease management and improve patient quality of life. Although oral therapy remains the mainstay of PD treatment, it is often associated with important limitations. Conventional oral formulations exhibit fluctuating plasma drug concentrations, undergo significant first-pass hepatic metabolism, and frequently produce gastrointestinal side effects [4]. These drawbacks result in variable clinical responses and necessitate frequent dosing, thereby affecting compliance, especially in elderly patients who constitute the majority of PD cases [5]. To address these challenges, transdermal drug delivery systems (TDDS) have been investigated as promising alternatives. Transdermal systems offer several advantages, including avoidance of gastrointestinal metabolism, reduction of hepatic first-pass effect, provision of controlled and sustained drug release, and improvement in patient adherence through reduced dosing frequency [6]. However, the development of efficient TDDS is complicated by the skin's highly organized stratum corneum, which functions as the principal barrier to drug permeation [7]. Thus, an effective transdermal formulation must not only maintain suitable mechanical and physicochemical properties but also incorporate safe and reversible penetration enhancers to facilitate drug transport across the skin. Rasagiline mesylate is a second-generation, selective, and irreversible inhibitor of monoamine oxidase-B (MAO-B) widely used in the symptomatic treatment of PD [8]. It offers neuroprotective benefits and enhances dopamine-related activity by reducing dopamine breakdown. Nevertheless, its oral administration is constrained by extensive hepatic metabolism, short elimination half-life (1.5–3 h), and variable bioavailability [9, 10].

These pharmacokinetic limitations may contribute to motor fluctuations and inconsistent clinical outcomes in PD patients. Designing a matrix-based transdermal delivery system for rasagiline could provide a means of maintaining steady therapeutic plasma levels, minimizing peak-trough variations, and reducing the frequency of administration, thereby improving both therapeutic efficacy and patient compliance [11]. The design of matrix diffusion-controlled patches involves the use of suitable polymers that can sustain drug release and ensure film integrity. Poly(meth)acrylate copolymers such as Eudragit® RL and RS have been widely employed as film formers because of their favorable mechanical properties, safety profile, and controlled release potential [12]. Plasticizers such as dibutyl phthalate are often incorporated to improve flexibility and reduce brittleness. To further enhance permeation, various penetration enhancers can be employed. These agents act by transiently disturbing the lipid organization of the stratum corneum, thereby increasing drug diffusivity [13]. Ideally, a

penetration enhancer should be pharmacologically inert, reversible in action, and non-irritant to the skin [14]. In this context, different classes of enhancers such as isopropyl myristate (a fatty acid ester), Span® 80 and Tween® 20 (non-ionic surfactants), eucalyptus oil (essential oil), and limonene (a terpene) have been investigated for their ability to increase percutaneous absorption [15, 16]. These agents, generally regarded as safe, have been shown to provide significant enhancement in skin permeability without causing permanent damage. Systematic evaluation of such enhancers in rasagiline matrix patches could therefore identify the most effective candidate capable of facilitating sustained therapeutic levels. The present study was designed to develop and characterize matrix diffusion-controlled transdermal patches of rasagiline. Particular emphasis was placed on optimizing the polymeric composition, evaluating physicochemical and mechanical properties, investigating drug–polymer compatibility, and assessing the impact of different permeation enhancers on skin penetration. By combining rational polymer selection with enhancer optimization, this work aims to provide a novel and effective transdermal system capable of improving rasagiline bioavailability and offering sustained therapeutic benefit in the management of Parkinson's disease.

MATERIALS AND METHODS

Materials

Rasagiline mesylate (RAS) was obtained as a gift sample from a pharmaceutical company. Poly(meth)acrylate-based polymers, Eudragit® RL 100 and Eudragit® RS 100, were purchased from Evonik Rohm GmbH, Germany. Polyvinyl alcohol (PVA, MW 75,000) was used to prepare the backing membrane (PanReac AppliChem, Spain). Dibutyl phthalate (DBP) was employed as a plasticizer (Merck, Germany). Solvents such as methanol and chloroform were of analytical grade. Permeation enhancers including isopropyl myristate (IPM), eucalyptus oil, Span® 80, Tween® 20, and limonene were procured from Sigma-Aldrich (St. Louis, USA), acetonitrile, HPLC grade, phosphate buffer pH 7.4. Distilled water was obtained in-house from a water distillation assembly.

Method

Preparation of RAS transdermal patches

Matrix transdermal patches of rasagiline were prepared by a solvent casting technique. The PVA backing membrane (4% w/v) was cast on glass Petri plates and dried at 40 °C for 4 h. Rasagiline, polymer blends (Eudragit RL 100:RS 100), and DBP were dissolved in a chloroform: methanol mixture (9:1 v/v) under sonication to obtain a uniform solution. The polymer ratios and enhancer concentrations were varied to prepare 15 different formulations (table 1).

The solution was poured over the pre-prepared PVA backing membrane, covered with inverted funnels to ensure controlled solvent evaporation, and dried in a hot air oven at 35 °C for 48 h. After drying, the patches were carefully removed, wrapped in aluminum foil, and stored in desiccators at room temperature for further analysis.

Table 1: Composition of rasagiline transdermal patch formulations

Formula	RAS (mg)	Eudragit RL: RS ratio	DBP (% w/w of polymer)	Enhancer type	Enhancer conc. (% w/w)	Solvent (v/v) CHCl3: MeOH
R1	5	9:1	30	IPM	2	9:1
R2	5	9:1	30	IPM	5	9:1
R3	5	9:1	30	IPM	10	9:1
R4	5	8:2	30	Eucalyptus oil	2	9:1
R5	5	8:2	30	Eucalyptus oil	5	9:1
R6	5	8:2	30	Eucalyptus oil	10	9:1
R7	5	7:3	30	Span® 80	2	9:1
R8	5	7:3	30	Span® 80	5	9:1
R9	5	7:3	30	Span® 80	10	9:1
R10	5	6:4	30	Tween® 20	2	9:1
R11	5	6:4	30	Tween® 20	5	9:1
R12	5	6:4	30	Tween® 20	10	9:1
R13	5	5:5	30	Limonene	2	9:1
R14	5	5:5	30	Limonene	5	9:1
R15	5	5:5	30	Limonene	10	9:1

RAS (mg): Rasagiline amount (active substance) in milligrams per formulation., Eudragit RL: RS Ratio: Ratio of Eudragit® RL 100 to Eudragit® RS 100 polymers used as film-forming agents., DBP (% w/w of polymer): Dibutyl phthalate concentration, expressed as percentage (weight/weight) of the total polymer weight; used as a plasticizer. Enhancer type: Type of permeation enhancer incorporated into the film formulation. IPM: Isopropyl myristate, Eucalyptus oil: Natural terpene-based penetration enhancer, Span® 80: Sorbitan monooleate (nonionic surfactant), Tween® 20: Polyoxyethylene sorbitan monolaurate (nonionic surfactant)

Drug content uniformity and assay

The uniform distribution of the active pharmaceutical ingredient (API) within the transdermal systems was assessed using a validated high-performance liquid chromatography (HPLC) method. An accurately cut portion of each patch (1.5 cm^2) was weighed and placed in a volumetric flask containing a mixture of methanol and phosphate buffer (pH 7.0, 1:1 v/v). The mixture was sonicated for 30 min to ensure complete extraction of the drug, followed by filtration through a 0.45 µm membrane filter. Chromatographic separation was achieved on a reversed-phase C18 column (150 × 4.6 mm, 5 µm) maintained at 30 °C. The mobile phase consisted of phosphate buffer (0.02 M, pH adjusted to 3.0 with orthophosphoric acid) and acetonitrile in a 70:30 ratio, delivered at a flow rate of 1.0 ml/min. The eluent was monitored at 228 nm using a UV detector, and an injection volume of 20 µl** was employed. Standard calibration curves were constructed over the range of 0.5–20 µg/ml, showing excellent linearity with a correlation coefficient (r^2) greater than 0.999. Drug content for each formulation was calculated based on the calibration curve, and results were expressed as percentage of the theoretical drug load. Ten patches from each batch were assayed individually to determine content uniformity [15. 17]

Characterization of rasagiline transdermal patches

Visual and physical assessment

All prepared polymeric rasagiline patches were examined visually for surface smoothness, flexibility, brittleness, stickiness, transparency, and uniformity. Any visible imperfections, such as cracks, bubbles, or uneven surfaces were noted.

Thickness measurement

The thickness of each patch was measured using a digital micrometer screw gauge (Sharp Fine Type-A, Zhejiang, China). Three randomly selected patches from each formulation were tested at three different points on each patch, and the mean thickness was calculated [17].

Weight uniformity

Three patches (1.5 cm^2 each) from each formulation were weighed on a digital analytical balance (Shimadzu AUX220, Kyoto, Japan). The average weight was determined to assess weight variation among formulations [17].

Folding endurance

The flexibility of patches was evaluated by repeatedly folding a 2×2 cm segment at the same point until the film fractured. Three patches per formulation were tested, and the average folding endurance was recorded [18].

Moisture content

To determine the moisture content, 1×1 cm film samples were weighed and stored in a desiccator containing silica gel at 25 °C. The patches were weighed daily until a constant weight was obtained. The percentage moisture content was calculated using the formula [18]:

$$\text{Moisture Content (\%)} = \frac{\text{Initial Weight} - \text{Final Weight}}{\text{Final Weight}} * 100$$

Moisture uptake

To evaluate hygroscopicity, 1×1 cm patches were weighed and placed in a desiccator with a saturated potassium chloride solution (84% RH) at 25 °C. The patches were weighed daily for 5 days or until weight stabilized. Moisture uptake was calculated as 17]:

$$\text{Moisture uptake (\%)} = \frac{\text{Final weight} - \text{Initial weight}}{\text{Initial weight}} * 100$$

Water vapor transmission and permeability

The water vapor transmission rate (WVTR) was determined using 1×1 cm films fixed over 5 ml vials containing $CaCl_2$ as desiccant. The vials were stored at 25 °C with 84% RH and weighed periodically. WVTR was calculated as [18]:

$$\text{Q} = \frac{\text{Final weight} - \text{Initial weight}}{\text{Time} * \text{Area}}$$

Water vapor permeability (WVP) was then calculated using:

$$\text{P} = \frac{\text{Q. d}}{\text{A. T. (S.}\frac{(\text{R1}-\text{R2})}{100})}$$

where dd = film thickness, AA = exposed area, TT = time, SS = saturated vapor pressure at test temperature, R1 = RH in chamber, R2 = RH inside vial.

Swelling behavior and percentage weight gain

To assess the swelling capacity, 1×1 cm films were weighed (W_1) and immersed in distilled water for 5, 10, 30, and 60 min. The swollen films were blotted and weighed immediately (W_2). The swelling index and percentage weight increase were calculated as [18]:

$$\text{Percent swelling index} = \frac{\text{W2} - \text{W1}}{\text{W1}} * 100$$

Characterization and Evaluation of Rasagiline Transdermal Patches Erosion assessment the percentage mass loss of prepared patches was determined to evaluate their erosion behavior. Film samples (1 × 1 cm) were dried overnight at 40±2 °C, affixed to pre-weighed glass coverslips, and reweighed. The slips were then immersed in distilled water contained in Petri dishes for 60 min. Subsequently, the samples were blotted, dried superficially, and reweighed. Films that underwent complete disintegration were excluded. The percentage erosion was calculated as [19]:

$$\text{Erosion \%} = \frac{\text{W2} - \text{W1}}{\text{W1}} * 100$$

where *W1* is the initial weight, and *W2* is the post-immersion weight.

Adhesive performance testing

The adhesive capacity of the transdermal films was evaluated using peel strength and tack tests. For the 180° peel test, strips of each formulation (25 × 100 mm) were fixed onto a standard substrate and peeled off using a universal testing machine (Instron, USA) at 300 mm/min. The mean force required for detachment (N/25 mm) was recorded. Tackiness was assessed by the probe tack method with a texture analyzer. A stainless-steel probe was pressed onto the adhesive surface under light force, held briefly, and withdrawn at 0.5 mm/s. The maximum detachment force was noted as the tack value. All measurements were performed at 25±2 °C and 50±5% RH [20].

Fourier transform infrared spectroscopy (FTIR)

FTIR analysis was employed to investigate possible drug–polymer or drug–excipient interactions. Spectra of pure rasagiline, individual polymers (Eudragit® RS100, RL100), and their physical mixtures were recorded in the 4000–600 cm^{-1} region using ATR-FTIR (Shimadzu IR Prestige 21). The data were processed with Opus software (Bruker, Germany) [21].

Differential scanning calorimetry (DSC)

Thermal behavior of rasagiline, polymers, and their binary blends was investigated using DSC (SDT Q600, TA Instruments, USA). Approximately 3–5 mg of sample was sealed in aluminum pans and heated under nitrogen at 20 °C/min within the range of 30–800 °C. The thermograms were analyzed for melting transitions, enthalpy changes, and possible interactions.

X-ray Diffraction (XRD) analysis

Crystallinity of rasagiline, blank films, and medicated patches was examined by powder XRD (PAN alytical X' Pert High Score Plus, Netherlands). Scans were performed with Cu-Kα radiation at 30 kV and 15 mA, over 2θ range of 2°–60°, with a step size of 0.02°.

Scanning electron microscopy (SEM)

Surface morphology before and after drug release was evaluated using SEM (Quanta 250, FEI, USA). Patches were mounted on aluminum stubs, sputter-coated with gold, and observed at suitable magnifications to study uniformity and porosity.

***In vitro* release testing**

Drug release studies were performed using the paddle-over-disc apparatus (USP type V). Patches (1.5 cm^2) were secured in disc assemblies and immersed in 500 ml phosphate buffer (pH 7.4), maintained at 32±1 °C with a paddle speed of 50 rpm. Aliquots (3 ml) were withdrawn at predetermined intervals (0.5–24 h), filtered, and analyzed spectrophotometrically at 227 nm. Withdrawn volumes were replaced with fresh medium. Release data were fitted to kinetic models (zero order, first order, Higuchi, and Korsmeyer–Peppas) to deduce release mechanisms [20, 21].

Ex vivo permeation studies

Rabbit abdominal skin was used as the diffusion membrane and was collected from healthy rabbits obtained from a licensed slaughterhouse following routine slaughter procedures, in accordance with institutional and ethical guidelines. Rabbit abdominal skin was selected as the ex vivo model for permeation studies because it exhibits histological and permeability characteristics comparable to human skin, particularly in terms of epidermal thickness and lipid composition. The rabbit model is widely used in pharmaceutical and transdermal formulation research due to its availability, ease of handling, and reproducibility of results. Furthermore, using excised animal skin provides a controlled, ethical alternative to *in vivo* testing while maintaining physiological relevance for diffusion and absorption studies.

Ethical approval for the use of animal tissues was obtained from the Institutional Animal Ethics Committee (IAEC) under approval reference number [CAE/2025/07]. All procedures were conducted following the guidelines for the care and use of laboratory animals. Skin Integrity Testing.

Before use, each skin sample was visually examined for cuts, abrasions, or subdermal damage. The integrity of the stratum corneum was confirmed by measuring the electrical resistance across the skin using a digital LCR meter (or equivalent device). Samples showing

resistance values above 20 kΩ cm^2 were considered intact and suitable for diffusion studies. Alternatively, trypan blue dye exclusion was used to confirm that the skin barrier remained unbroken; any samples showing dye penetration were discarded.

Skin preparation involved depilation, excision, and storage at −20 °C until use. Permeation studies were conducted in Franz diffusion cells (diffusion area 1.5 cm^2; receptor volume 12 ml), maintained at 32±1 °C with continuous stirring at 120 rpm. Patches (1.5 cm^2) were placed on the stratum corneum side, and receptor compartments filled with phosphate buffer (pH 7.4). Samples (1 ml) were withdrawn at intervals up to 24 h, replacing with fresh buffer each time. Drug content was quantified by UV spectrophotometry [22].

Kinetic modeling of permeation data

The cumulative amount of drug permeated per unit area (Qn) was calculated and plotted against time to determine flux and permeability coefficients. The corrected concentrations were derived to account for sample withdrawal. Mathematical models, including Higuchi and Korsmeyer–Peppas equations, were applied to interpret the release mechanism (Fickian vs. non-Fickian diffusion) [23, 24].

Statistical analysis

All experiments were performed in triplicate. Results are expressed as mean±SD. Comparisons between formulations were performed using one-way ANOVA followed by post hoc tests (LSD), with significance levels set at $p<0.05$ and $p<0.01$.

RESULTS AND DISCUSSION

Physical characterization

Results of physical evaluation are summarized in table 2. All rasagiline-loaded polymeric films were found to be flexible, transparent, and non-brittle. Formulations containing higher ratios of Eudragit® RS 100 appeared slightly sticky, yet retained desirable physical uniformity. Blank patches were comparatively less sticky than drug-loaded patches. The PVA backing membrane remained firmly attached to the matrix layer, confirming mechanical stability of the system [25]

The thickness of the prepared films ranged between 182–188 µm, while the average weight of a 1.5 cm^2 patch was within 32.1–33.6 mg, indicating uniform distribution of drug and excipients. Folding endurance values exceeded 200 folds for all formulations, reflecting excellent flexibility and resistance to brittleness. Drug content was consistent, ranging from 97.88% to 99.11%, demonstrating uniform drug incorporation.

Moisture content of the formulations was low (4.58%–5.02%), an attribute that favors long-term stability by reducing microbial contamination risk and preventing bulkiness. The moisture uptake values (5.92%–6.48%) were influenced by the hydrophilic polymer content, with higher uptake observed in formulations rich in hydrophilic polymers. In contrast, films with a higher proportion of Eudragit RS 100 demonstrated reduced swelling and water vapor transmission due to the hydrophobic nature of the polymer, thereby enhancing patch integrity. The swelling index values were confined to a narrow range (1.05–1.21), indicating controlled hydration behavior and limited dimensional expansion of the polymeric films. This minimal variation, despite changes in polymer ratio, can be attributed to the short immersion duration (15 min) used in the swelling study, which likely allowed the system to reach an early equilibrium state, thereby reducing the sensitivity of the method to compositional differences. Additionally, the polymers employed exhibit inherently restricted water uptake at equilibrium, and the presence of intermolecular interactions and partial cross-linking within the polymeric matrix may have further constrained polymer chain relaxation and pore expansion. Collectively, these factors limited differential swelling responses among formulations, resulting in closely comparable swelling index values [26–28].

Table 2: Physicochemical properties of rasagiline transdermal matrix patches

Code	Appearance[a]	Thickness (µm) ±SD	Weight (mg/1.5 cm^2) ±SD	Folding endurance ±SD	Moisture content (%)	Moisture uptake (%)	Swelling index (%)	Erosion (%)	WVP ($mg \cdot Pa^{-1} \cdot cm^{-1} \cdot h^{-1}$)	WVTR ($g/m^2 \cdot h$)	Drug content (%) ±SD
R1	Ss, F, NB, T, St, H	182±2.1	32.1±0.21	>200	4.76	6.12	1.12	5.15	6.78×10^{-5}	3.92×10^{-5}	98.21±0.35
R2	Ss, F, NB, T, St, H	185±1.9	33.0±0.18	>200	4.89	6.25	1.05	5.32	7.01×10^{-5}	4.11×10^{-5}	97.88±0.42
R3	Ss, F, NB, T, St, H	184±2.4	32.5±0.25	>200	5.02	6.48	1.08	5.28	6.91×10^{-5}	3.85×10^{-5}	99.12±0.28
R4	Ss, F, NB, T, St, H	186±1.7	33.2±0.32	>200	4.61	5.92	1.21	5.05	7.15×10^{-5}	4.22×10^{-5}	98.66±0.39
R5	Ss, F, NB, T, St, H	183±2.2	32.8±0.27	>200	4.75	6.08	1.17	5.42	6.88×10^{-5}	3.97×10^{-5}	97.94±0.41
R6	Ss, F, NB, T, St, H	185±1.6	33.1±0.19	>200	4.92	6.37	1.14	5.23	7.02×10^{-5}	4.15×10^{-5}	98.77±0.36
R7	Ss, F, NB, T, St, H	182±2.0	32.7±0.23	>200	4.58	5.99	1.19	5.34	6.75×10^{-5}	3.89×10^{-5}	99.04±0.29
R8	Ss, F, NB, T, St, H	187±1.8	33.4±0.21	>200	4.83	6.22	1.16	5.48	7.08×10^{-5}	4.20×10^{-5}	98.55±0.38
R9	Ss, F, NB, T, St, H	184±2.3	32.9±0.28	>200	4.69	6.14	1.11	5.37	6.84×10^{-5}	3.94×10^{-5}	97.99±0.33
R10	Ss, F, NB, T, St, H	188±1.9	33.6±0.24	>200	4.91	6.28	1.13	5.41	7.12×10^{-5}	4.19×10^{-5}	98.62±0.37
R11	Ss, F, NB, T, St, H	183±2.5	32.6±0.20	>200	4.72	6.05	1.09	5.29	6.89×10^{-5}	3.95×10^{-5}	98.03±0.34
R12	Ss, F, NB, T, St, H	186±2.2	33.3±0.26	>200	5.01	6.41	1.15	5.44	7.06×10^{-5}	4.18×10^{-5}	98.85±0.31
R13	Ss, F, NB, T, St, H	182±1.8	32.4±0.22	>200	4.67	6.02	1.10	5.26	6.77×10^{-5}	3.91×10^{-5}	97.91±0.36
R14	Ss, F, NB, T, St, H	185±2.0	33.0±0.25	>200	4.80	6.20	1.18	5.39	7.00×10^{-5}	4.10×10^{-5}	98.48±0.32
R15	Ss, F, NB, T, St, H	187±2.3	33.5±0.29	>200	4.95	6.30	1.20	5.51	7.09×10^{-5}	4.21×10^{-5}	99.11±0.30

Notes: Each value is the mean±SD (n=7 for thickness; n=3 for other parameters). Folding endurance refers to the number of times the patch could be folded without breaking. Abbreviations: Ss, surface smoothness; F, flexibility; NB, non-brittle; T, transparent; St, sticky; H, homogeneous; SD, standard deviation; WVP, water vapor permeability; WVTR, water vapor transmission rate.

FTIR spectroscopic analysis

FTIR spectra of pure rasagiline exhibited characteristic peaks at 3,336 cm^{-1} (N–H stretching), 1,716 cm^{-1} (C=O stretching), 1,448 cm^{-1} (C–N stretching), and 1,105 cm^{-1} (C–O stretching). These characteristic peaks were also present in the drug–polymer formulations, without any significant shift or disappearance, indicating the absence of chemical incompatibility between rasagiline and the selected polymers. This confirmed that rasagiline was physically dispersed in the polymeric matrix without chemical interaction (fig. 1) [29].

SEM analysis

The surface morphology of optimized rasagiline patches was studied using SEM. The micrographs revealed a relatively smooth surface with small, irregularly distributed pores, which were attributed to the leaching of hydrophilic components during the release process. The films maintained their elasticity even after drug release, with no visible cracks or brittleness. Similar porous surface morphology after drug release has been reported by previous studies on polymeric transdermal films containing hydrophilic–hydrophobic blends. These findings confirm that the films retained mechanical stability while permitting controlled drug diffusion (fig. 2) [30].

XRD studies

X-ray diffraction analysis was performed to assess the physical state of rasagiline within the polymeric films. Pure rasagiline displayed sharp crystalline peaks at 2θ values of 12.8°, 18.6°, and 20.9°, characteristic of its crystalline nature. However, the diffractograms

of the drug-loaded films exhibited broad peaks with markedly reduced intensity, suggesting conversion of the drug into an amorphous or molecularly dispersed state within the polymeric network. This transition from crystalline to amorphous form is desirable, as it enhances drug solubility and facilitates sustained release (fig. 3) [31, 32].

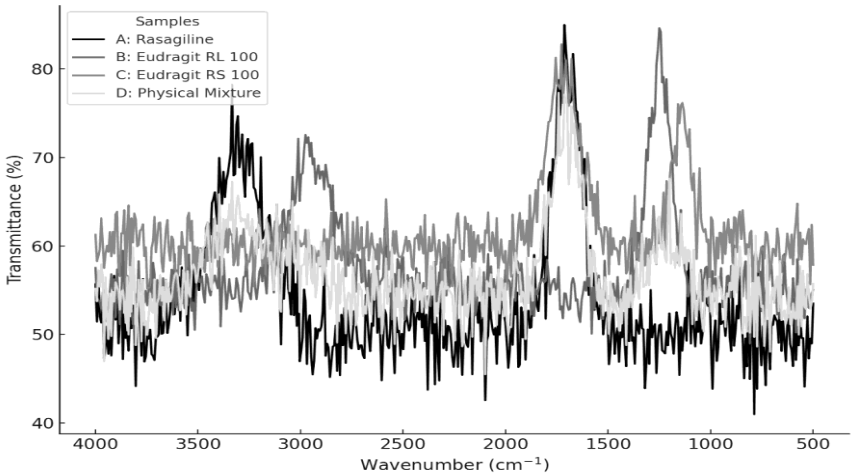

Fig. 1: FTIR spectra of Rasagiline film formulations obtained experimentally using FTIR spectroscopy

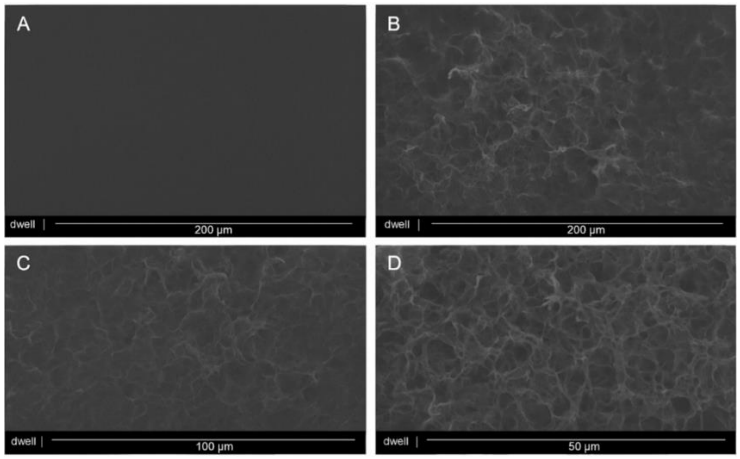

Fig. 2: SEM images acquired experimentally to study surface morphology (A) polymeric patch surface prior to permeation at 200 µm, (B) patch matrix after permeation study at 200 µm, (C) patch morphology after permeation study at 100 µm, and (D) patch morphology after permeation study at 50 µm

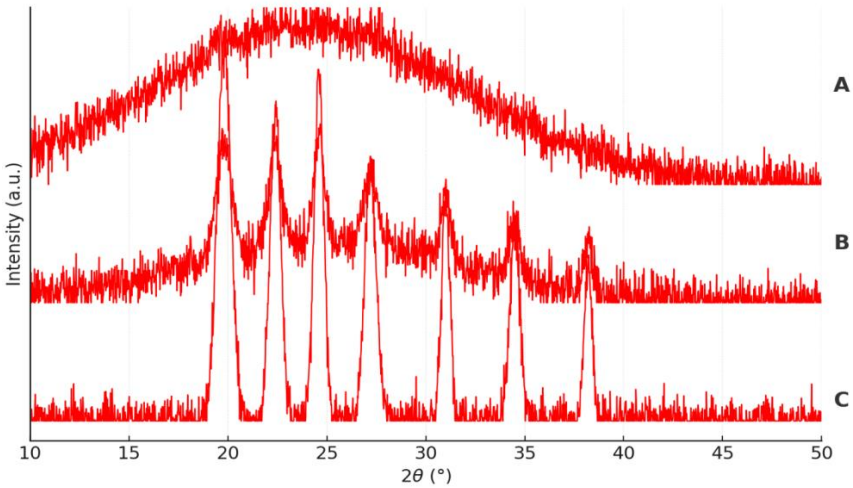

Fig. 3: Ray diffractograms of (A) rasagiline-loaded polymeric patches, (B) physical mixture of rasagiline, Eudragit® RS 100, and Eudragit® RL 100, and (C) pure rasagiline

Adhesive performance testing

The adhesive behavior of rasagiline-loaded transdermal patches was evaluated to assess their capacity to remain attached to the skin surface without detachment or irritation (fig. 4, table 3). All formulations exhibited acceptable adhesion, although differences were observed depending on the polymer matrix. Patches containing a higher proportion of Eudragit® RS 100 demonstrated greater adhesion, attributed to the inherent tackiness of this hydrophobic polymer. Peel adhesion strength was measured in the range of 120–185 g/cm^2, while tack force values were between 85–142 g/cm^2. Among the tested batches, R4, R5, R7, R8, R11, and R13 exhibited superior adhesive properties, maintaining adequate stickiness for the full 24-h evaluation period without producing signs of skin irritation. These results suggest that the relative ratio of hydrophilic to hydrophobic polymers is a key determinant of adhesive performance. The optimized patches achieved an appropriate balance of adhesion and flexibility, promoting patient comfort while minimizing the likelihood of premature detachment [33-35].

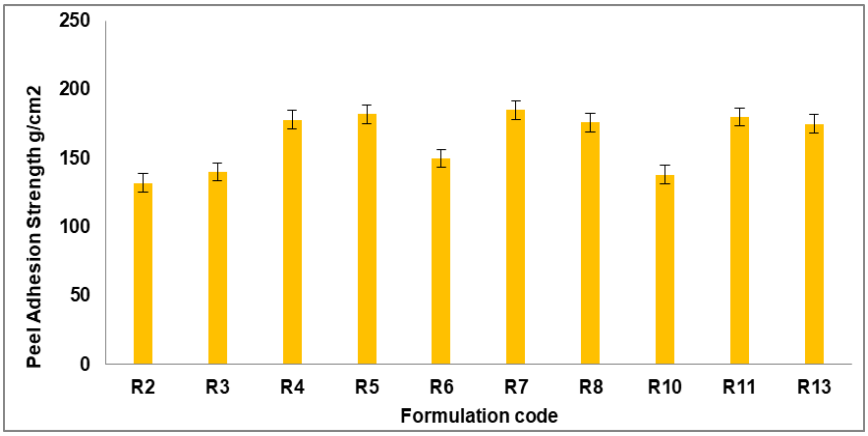

Fig. 4: Adhesive performance (peel adhesion, g/cm^2) for the best formulations. Error bars indicated SD values

Table 3: Peel adhesion strength of rasagiline film formulations

Formulation code	Peel adhesion strength (g/cm^2, mean±SD)
R2	132.4±4.6
R3	140.2±5.1
R4	177.3±6.3
R5	181.2±5.8
R6	150.4±6.0
R7	188.6±7.1
R8	175.5±5.9
R10	137.8±4.8
R11	180.3±6.2
R13	170.8±5.7

Value are expressed as mean±standard deviation (SD). Peel adhesion strength was measured in g/cm^2 using a standardized peel adhesion test. Each value represents the average of three independent determinations (n = 3). All formulations were evaluated under identical experimental conditions

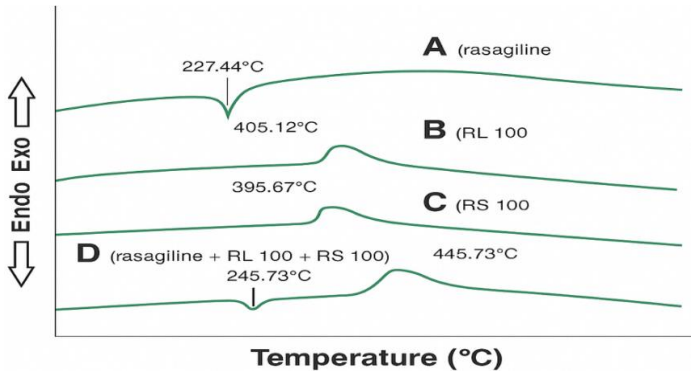

Fig. 5: DSC thermograms recorded experimentally for Rasagiline-loaded films. (A) Rasagiline, (B) Eudragit RL100, (C) Eudragit RS 100, and (D) Physical mixture

Differential scanning calorimetry (DSC)

DSC analysis was performed to verify the thermal behavior, identity, and purity of Rasagiline. The thermogram of pure Rasagiline displayed a sharp endothermic peak at 183.5 °C (fig. 5), with an onset at 178.9 °C, which corresponds well with the melting point values reported in previous literature. The slight shift in melting point (183.5 °C → 182.7 °C) is indicative of a minor drug–polymer

interaction or a dilution effect, which may reduce crystal lattice energy without indicating chemical incompatibility. Similar findings were observed by earlier studies, confirming the crystalline nature of the drug. The physical mixture of Rasagiline with Eudragit® RL 100 and Eudragit® RS 100 demonstrated an endothermic event at 182.7 °C, closely matching the pure drug, suggesting no significant interaction between the drug and the polymers [36].

In vitro release studies

In vitro dissolution experiments were conducted to evaluate the influence of polymeric composition on the release kinetics of Rasagiline from matrix-type transdermal patches and to determine the most suitable formulation for extended delivery over 24 h. The study was performed using a USP dissolution apparatus V (paddle-over-disc method), with experiments lasting 24 h. Aliquots were collected at predetermined intervals and analyzed spectrophotometrically for Rasagiline content using a previously validated calibration curve.

The cumulative percentage of drug released from patches R1–R15 was calculated, and release profiles were plotted against time. Among the prepared formulations, batch R7, containing a 7:3 ratio of Eudragit RL 100 to Eudragit RS 100, demonstrated the highest cumulative drug release compared to other polymeric blends. This observation suggests that the release behavior was strongly influenced by the relative proportions of the two methacrylate copolymers.

Eudragit RS 100, known for its low permeability, acted as a release-retarding polymer, thereby limiting drug diffusion through the matrix. In contrast, Eudragit RL 100, which contains a higher proportion of quaternary ammonium groups and is more hydrophilic, enhanced water penetration and facilitated drug diffusion. Thus, formulations containing greater proportions of RL 100 exhibited faster and more extended release, while those with higher RS 100 content showed a significantly slower release profile ($p<0.05$). These results highlight the crucial role of polymer selection in tailoring drug release performance.

Formulations incorporating the 7:3 ratio of RL 100 to RS 100 were further evaluated with various permeation enhancers, namely isopropyl myristate (IPM), Span® 80, Tween® 20, eucalyptus oil, and limonene at three different concentrations. The addition of enhancers substantially improved the release rate of rasagiline. The effect of each enhancer and its concentration is presented in fig. 6A–E, while fig. 6F provides a comparative overview of the most effective enhancer levels. Among the tested options, the formulation containing 10% IPM achieved the maximum drug release (92.34% after 24 h), whereas the formulation without any enhancer exhibited the lowest release (52.41%) (fig. 6) [37-40].

The enhanced performance of IPM may be attributed to its lipophilic nature and its ability to disrupt lipid domains, thereby increasing hydration and diffusivity within the polymeric matrix. Similarly, eucalyptus oil and Span® 80 were found to improve Rasagiline release significantly, possibly due to their dual effect on polymer plasticization and barrier modification. In contrast, Tween® 20 and limonene exhibited moderate enhancing potential [41].

Mechanistically, the Rasagiline release process was governed by the structural characteristics of the polymeric film. The relatively porous network formed by RL 100 facilitated solvent penetration, resulting in drug leaching and the creation of microchannels that enhanced sustained diffusion. RS 100, on the other hand, contributed to matrix rigidity and acted as a diffusion barrier. Together, these polymers created a balance between sustained and controlled release [40].

Drug release kinetics

Kinetic analysis was performed by fitting release data into different mathematical models, including zero-order, first-order, Higuchi, and Korsmeyer–Peppas equations. The correlation coefficient values (R^2 = 0.963–0.998) indicated that the release followed predominantly the Higuchi model, consistent with diffusion-controlled transport. The calculated diffusion exponent (n) from the Korsmeyer–Peppas model ranged between 0.57–0.82, suggesting anomalous (non-Fickian) transport, where both diffusion and polymer relaxation mechanisms played a role. Notably, formulation R7 (RL 100: RS 100 in 7:3 ratio with 10% IPM) exhibited the highest Higuchi rate constant, confirming its suitability for sustained Rasagiline delivery [42].

Based on these findings, the optimized patch demonstrated the ability to extend Rasagiline release for 24 h in a controlled manner, thereby offering a promising strategy for improving patient compliance in long-term Parkinson's therapy (table 3).

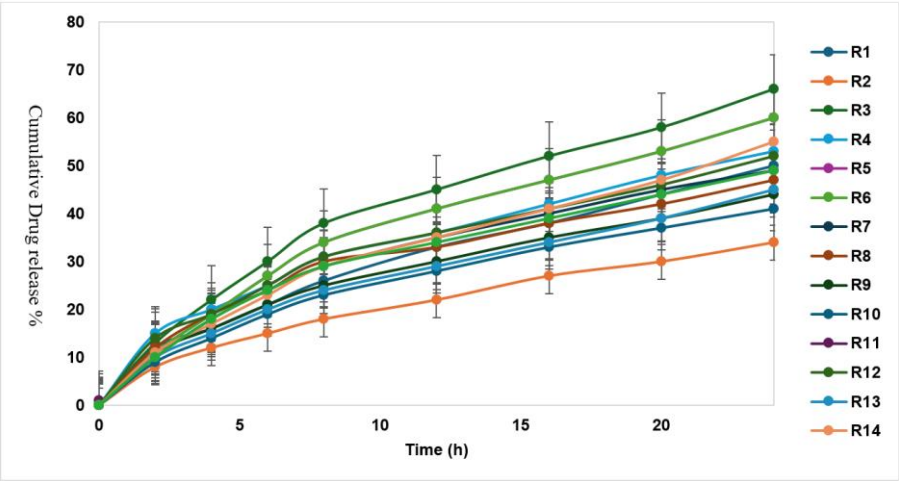

Fig. 6: Cumulative percentage of drug release versus time of different rasagiline transdermal patch formulations. Error bars indicated SD values

Ex vivo permeation studies

Ex vivo permeation experiments were conducted using a Franz diffusion cell to simulate drug transport across biological membranes and to predict *in vivo* absorption of Rasagiline. Excised rabbit skin was used as the diffusion barrier. The influence of penetration enhancers on drug permeation was investigated by incorporating five enhancers—isopropyl myristate (IPM), Span® 80, Tween® 20, eucalyptus oil, and limonene—at three concentration levels.

The permeation profiles demonstrated that enhancer incorporation significantly improved drug transport across the skin. The permeation flux (J), cumulative permeated amount at 24 h (Q_24), and enhancement factor (EF) for each formulation were calculated and are summarized in table 5 [45].

Among the tested enhancers, IPM at 10% w/w exhibited the highest permeation flux and enhancement factor, resulting in the maximum Rasagiline transport across the skin. In contrast, formulations lacking enhancers showed the lowest permeation, confirming the crucial role of permeation promoters in optimizing Rasagiline delivery from transdermal patches.

Effect of permeation enhancers

The impact of various penetration enhancers on the percutaneous absorption of Rasagiline was expressed in terms of the enhancement factor (EF). Among the tested enhancers, isopropyl myristate (IPM) at 10% w/w exhibited the most pronounced effect, producing a 5.4-fold increase in permeation flux compared to the control formulation ($p<0.05$). In addition, the same formulation showed the highest cumulative drug permeation after 24 h (Q24 = 1,285.6 ng/cm^2; p = 0.021). At lower concentrations (2% w/w), the enhancement order was observed as IPM>eucalyptus oil>Span® 80>Tween® 20>limonene (fig. 8). At 5% w/w concentration, the order slightly changed to eucalyptus oil>IPM>Span® 80>Tween® 20>limonene (fig. 9). At higher levels (10% w/w), IPM again emerged as the most efficient enhancer, followed by eucalyptus oil>Span® 80>Tween® 20>limonene (fig. 7) [44, 45].

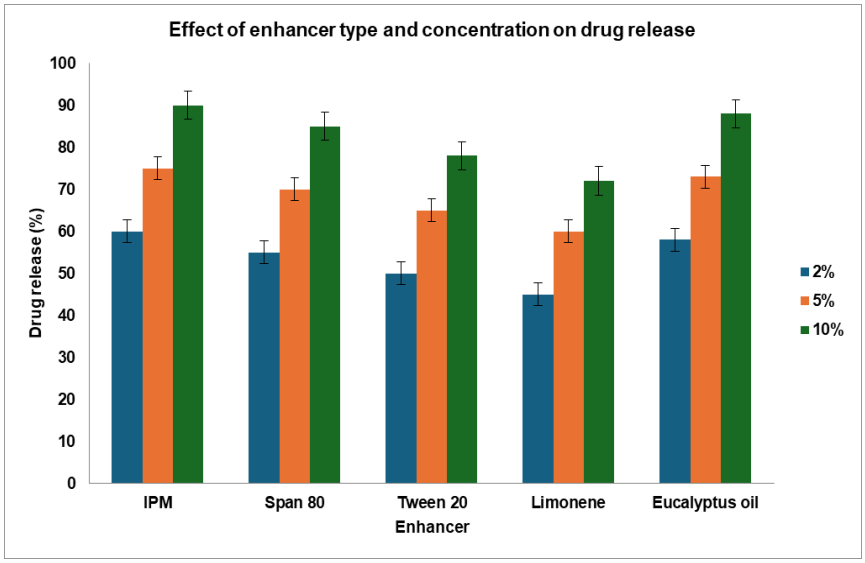

Fig. 7: Effect of different permeation enhancers and their concentrations on drug release from the formulated system, including isopropyl myristate, Span® 80, Tween® 20, limonene, and eucalyptus oil, with a comparison of the optimal enhancer levels showing maximum drug release (mean±SD). Abbreviations: IPM, isopropyl myristate; Euc, eucalyptus

The mechanism of action of IPM may be attributed to its ability to disrupt the tightly packed lipid bilayers of the stratum corneum, thereby improving skin permeability. Being moderately lipophilic, IPM can penetrate the lipid domains and simultaneously partition into the protein-rich polar regions, enhancing Rasagiline's solubility and diffusivity. As an aliphatic ester, it also increases the drug–skin partition coefficient and facilitates drug flux. Other enhancers demonstrated complementary effects. Eucalyptus oil exhibited strong permeation-promoting activity, consistent with earlier findings that it can significantly enhance dermal penetration of various small molecules. Span® 80, a hydrophobic surfactant with a low HLB value, increased Rasagiline transport by disturbing barrier function and altering the drug–stratum corneum partitioning. Tween® 20, a hydrophilic nonionic surfactant, primarily enhanced permeation by improving hydration of the stratum corneum, thus facilitating drug diffusion. Limonene, a terpene hydrocarbon, acted through lipid extraction from skin layers, which created additional diffusion pathways for drug transport (fig. 8, table 4) [33, 37].

Table 4: The effect of using different skin permeation enhancers on permeation of rasagiline across rabbit skin from patches

Formulation (Enhancer)	Cumulative drug permeated Q24 (ng/1.5 cm^2)	Permeation flux J (ng/cm^2/hr)	Enhancement factor
IPM 2%	1,120.35	47.52	5.12
IPM 5%	1,215.68	49.87	5.37
IPM 10%	1,342.92	53.71	5.78
Span® 80 2%	995.41	38.94	4.15
Span® 80 5%	1,042.16	40.62	4.34
Span® 80 10%	1,110.83	42.18	4.51
Tween® 20 2%	950.27	31.26	3.47
Tween® 20 5%	978.65	32.41	3.61
Tween® 20 10%	1,065.39	36.11	3.89
Eucalyptus oil 2%	1,078.42	39.12	4.27
Eucalyptus oil 5%	1,156.89	42.56	4.65
Eucalyptus oil 10%	1,188.57	43.78	4.73
Limonene 2%	765.18	24.39	2.71
Limonene 5%	846.92	27.87	3.12
Limonene 10%	910.64	30.87	3.43
Without enhancer	220.00	9.00	1.00

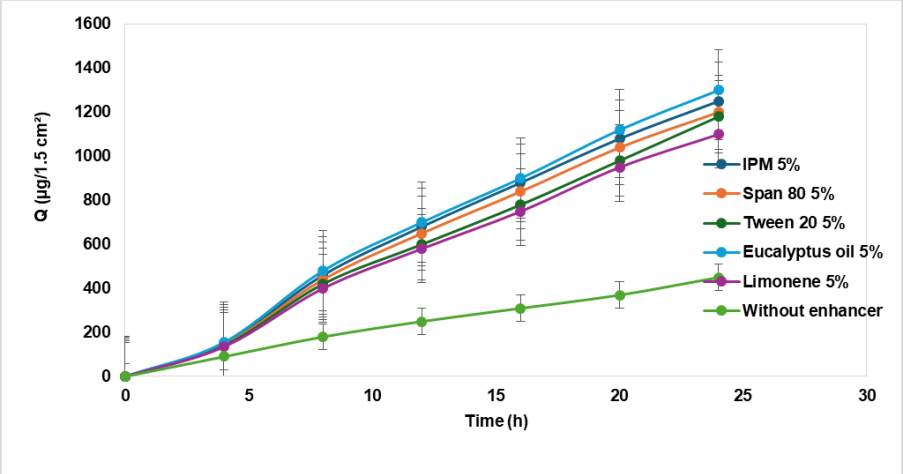

Fig. 8: Enhancement effect of different permeation enhancers on rasagiline permeation at 5% (w/w) concentration, Abbreviations: IPM, isopropyl myristate; Q, cumulative drug permeated

Table 5: Release kinetics of rasagiline from matrix patches having different ratios of polymers

Formulation code	Polymer ratios RL: RS	Zero order (r^2)	First order (r^2)	Higuchi (r^2)	Higuchi (K_H)	Korsmeyer–Peppas (r^2)	Korsmeyer–Peppas (n)
R1	9:1	0.9632	0.9715	0.9856	6.42	0.9868	0.582
R2	9:1	0.9695	0.9780	0.9872	6.88	0.9874	0.601
R3	9:1	0.9723	0.9825	0.9904	7.36	0.9886	0.615
R4	8:2	0.9708	0.9794	0.9885	7.01	0.9880	0.593
R5	8:2	0.9735	0.9810	0.9896	7.48	0.9892	0.609
R6	8:2	0.9752	0.9836	0.9912	7.89	0.9898	0.621
R7	7:3	0.9778	0.9855	0.9934	10.82	0.9916	0.652
R8	7:3	0.9765	0.9840	0.9926	9.74	0.9910	0.639
R9	7:3	0.9789	0.9862	0.9930	9.98	0.9918	0.667
R10	6:4	0.9712	0.9796	0.9889	6.55	0.9875	0.574
R11	6:4	0.9738	0.9818	0.9905	6.92	0.9887	0.596
R12	6:4	0.9750	0.9833	0.9918	7.24	0.9895	0.612
R13	5:5	0.9690	0.9774	0.9877	5.89	0.9869	0.584
R14	5:5	0.9705	0.9790	0.9889	6.10	0.9876	0.605
R15	5:5	0.9728	0.9812	0.9901	6.34	0.9883	0.624

CONCLUSION

Transdermal patches of rasagiline were successfully prepared using different ratios of methacrylate copolymer blends (RS 100 and RL 100). The optimized formulation containing a 7:3 ratio of RL 100 to RS 100 demonstrated the most desirable balance between flexibility, controlled release, and drug permeability.

Among the penetration enhancers investigated, IPM at 10% w/w provided the most effective enhancement in terms of both flux and total drug permeation across the skin. The kinetic analysis confirmed that drug release predominantly followed the Higuchi diffusion model, while Korsmeyer–Peppas analysis suggested a non-Fickian mechanism, indicating a combined effect of diffusion and polymer relaxation. These findings highlight that the use of methacrylate copolymer-based patches, combined with suitable enhancers such as IPM, offers a promising platform for the sustained transdermal delivery of Rasagiline. Such formulations may be particularly advantageous for patients who are unable to tolerate oral dosing, ensuring prolonged and controlled therapeutic effect.

Dalia A. Gaber conceptualized and designed the study, supervised all experimental work, analyzed and interpreted the data, and drafted the manuscript. Mostafa A. Mohamed contributed to experimental execution and data collection. Eman Al-Johani assisted in methodology development and manuscript review. Mohammed A. Amin and Siham Abdoun supported data analysis, technical validation, and critical revision of the manuscript.

FUNDING

Nil

AUTHORS CONTRIBUTIONS

All authors have contributed equally

CONFLICT OF INTERESTS

Declared none

REFRENCES

1. Saoji SD, Atram SC, Dhore PW, Deole PS, Raut NA, Dave VS. Influence of the component excipients on the quality and functionality of a transdermal film formulation. AAPS PharmSciTech. 2015;16(6):1344-56. doi: 10.1208/s12249-015-0322-0, PMID 25922089.
2. Parhi R, Suresh P. Transdermal delivery of diltiazem HCl from matrix film: effect of penetration enhancers and study of antihypertensive activity in rabbit model. J Adv Res. 2016;7(3):539-50. doi: 10.1016/j.jare.2015.09.001, PMID 27222758.
3. Rong X, Yang J, Ji Y, Zhu X, Lu Y, Mo X. Biocompatibility and safety of insulin-loaded chitosan nanoparticles/ PLGA-PEG-PLGA hydrogel (ICNPH) delivered by subconjunctival injection in rats. J Drug Deliv Sci Technol. 2019;49:556-62. doi: 10.1016/j.jddst.2018.12.032.
4. Salve PS, Gupta RR. Ex vivo skin permeation studies of sumatriptan succinate using different solvent systems and comparison with PLGA nanoparticles. J Drug Deliv Ther. 2019;9(4-S):59-67. doi: 10.22270/jddt.v9i4-s.3247.
5. Todo H. Transdermal permeation of drugs in various animal species. Pharmaceutics. 2017;9(3):33. doi: 10.3390/pharmaceutics9030033, PMID 28878145.

6. Joshi R, Garud N. Development optimization and characterization of flurbiprofen matrix transdermal drug delivery system using box–behnken statistical design. Futur J Pharm Sci. 2021;7(1):23. doi: 10.1186/s43094-021-00199-2.
7. Assaf SM, Ghanem AM, Alhaj SA. Formulation and evaluation of Eudragit® RL polymeric double-layer films for prolonged transdermal delivery of tamsulosin hydrochloride. Eur J Pharm Biopharm. 2023;186:122–31. doi: 10.1016/j.ejpb.2023.03.024.
8. Jeong WY, Kwon M, Choi HE, Kim KS. Recent advances in transdermal drug delivery systems: a review. Biomater Res. 2021;25(1):24. doi: 10.1186/s40824-021-00226-6, PMID 34321111.
9. Alkilani AZ, Nasereddin J, Hamed R, Nimrawi S, Hussein G, Abo Zour H. Beneath the skin: a review of current trends and future prospects of transdermal drug delivery systems. Pharmaceutics. 2022;14(6):1152. doi: 10.3390/pharmaceutics14061152, PMID 35745725.
10. Salih OS, Al-Akkam EJ. Microneedles as a promising technology to facilitate transdermal drug delivery. Int J Drug Deliv Technol. 2022;12(2):76-82. doi: 10.25258/ijddt.12.2.76.
11. Ruan S, Zhang Y, Feng N. Microneedle-mediated transdermal nanodelivery systems: a review. Biomater Sci. 2021;9(24):8065-89. doi: 10.1039/D1BM01249E, PMID 34752590.
12. Nainggolan AD, Anjani QK, Hartrianti P, Donnelly RF, Kurniawan A, Ramadon D. Microneedle-mediated transdermal delivery of genetic materials stem cells and secretome: an update and progression. Pharmaceutics. 2023;15(12):2767. doi: 10.3390/pharmaceutics15122767, PMID 38140107.
13. Abou El-Naga HM, El-Hashash SA, Yasen EM, Leporatti S, Hanafy NA. Starch-based hydrogel nanoparticles loaded with polyphenolic compounds of Moringa Oleifera leaf extract have hepatoprotective activity in bisphenol a-induced animal models. Polymers (Basel). 2022;14(14):2846. doi: 10.3390/polym14142846, PMID 35890622.
14. Karve T, Dandekar A, Agrahari V, Melissa Peet M, Banga AK, Doncel GF. Long-acting transdermal drug delivery formulations: current developments and innovative pharmaceutical approaches. Adv Drug Deliv Rev. 2024;210:115326. doi: 10.1016/j.addr.2024.115326, PMID 38692457.
15. Repka MA, Bandari S, Kallakunta VR, Vo AQ, McFall H, Pimparade MB. Melt extrusion with poorly soluble drugs an integrated review. Int J Pharm. 2018;535(1-2):68-85. doi: 10.1016/j.ijpharm.2017.10.056, PMID 29102700.
16. Song C, Repka MA. Hot-melt extrusion technology for transdermal patch development. Drug Dev Ind Pharm. 2018;44(8):1080-93. doi: 10.1080/03639045.2018.1476834.
17. Kochhar JS, Tan JJ, Kwang YC, Kang L. Introduction & literature review. In: Tan JJ, Kang LC, editors. Microneedles for transdermal drug delivery. Berlin: Springer; 2019. p. 1-30. doi: 10.1007/978-3-030-15444-8_1.
18. Patel RP, Patel G, Baria A. Formulation and evaluation of transdermal drug delivery system: a review. Int J Pharm Pharm Sci. 2009;1(1):1-7.
19. Jayaprakash R, Hameed J, Anupriya A. Transdermal drug delivery. Asian J Pharm Clin Res. 2017;10(10):36-40. doi: 10.22159/ajpcr.2017.v10i10.19909.
20. Shingade GM. Review on: recent trend on transdermal drug delivery system. J Drug Delivery Ther. 2012;2(1):66-75. doi: 10.22270/jddt.v2i1.74.
21. Bakhrushina EO, Shumkova MM, Avdonina YV, Ananian AA, Babazadeh M, Pouya G. Transdermal drug delivery systems: methods for enhancing skin permeability and their evaluation. Pharmaceutics. 2025;17(7):936. doi: 10.3390/pharmaceutics17070936, PMID 40733144.
22. Kathe K, Kathpalia H. Film-forming systems for topical and transdermal drug delivery. Asian J Pharm Sci. 2017;12(6):487-97. doi: 10.1016/j.ajps.2017.07.004, PMID 32104362.
23. Szunerits S, Boukherroub R. Heat: a highly efficient skin enhancer for transdermal drug delivery. Front Bioeng Biotechnol. 2018;6:15. doi: 10.3389/fbioe.2018.00015, PMID 29497609.
24. Parhi R, Mandru A. Enhancement of skin permeability with thermal ablation techniques: concept to commercial products. Drug Deliv Transl Res. 2021;11(3):817-41. doi: 10.1007/s13346-020-00823-3, PMID 32696221.
25. Babaie S, Del Bakhshayesh AR, Ha JW, Hamishehkar H, Kim KH. Invasome: a novel nanocarrier for transdermal drug delivery. Nanomaterials (Basel). 2020;10(2):341. doi: 10.3390/nano10020341, PMID 32079276.
26. Zhang Z, Liu Y, Chen Y, Li L, Lan P, He D. Transdermal delivery of 5-aminolevulinic acid by nanoethosome gels for photodynamic therapy of hypertrophic scars. ACS Appl Mater Interfaces. 2019;11(4):3704-14. doi: 10.1021/acsami.8b17498, PMID 30589527.
27. Amjadi M, Mostaghaci B, Sitti M. Recent advances in skin penetration enhancers for transdermal gene and drug delivery. Curr Gene Ther. 2017;17(2):139-46. doi: 10.2174/1566523217666170510151540, PMID 28494734.
28. Radmard A, Banga AK. Microneedle-assisted transdermal delivery of lurasidone nanoparticles. Pharmaceutics. 2024;16(3):308. doi: 10.3390/pharmaceutics16030308, PMID 38543202.
29. Das A, Ahmed AB. Formulation and evaluation of transdermal patch of indomethacin containing patchouli oil as natural penetration enhancer. Asian J Pharm Clin Res. 2017;10(11):320. doi: 10.22159/ajpcr.2017.v10i11.20926.
30. Karve T, Dandekar A, Agrahari V, Melissa Peet M, Banga AK, Doncel GF. Long-acting transdermal drug delivery formulations: current developments and innovative pharmaceutical approaches. Adv Drug Deliv Rev. 2024;210:115326. doi: 10.1016/j.addr.2024.115326, PMID 38692457.
31. Meng F, Qiao X, Xin C, Ju X, He M. Recent progress of polymeric microneedle-assisted long-acting transdermal drug delivery. J Pharm Pharm Sci. 2024;27:12434. doi: 10.3389/jpps.2024.12434, PMID 38571937.
32. Repka MA, Bandari S, Kallakunta VR, Vo AQ, McFall H, Pimparade MB. Melt extrusion with poorly soluble drugs an integrated review. Int J Pharm. 2018;535(1-2):68-85. doi: 10.1016/j.ijpharm.2017.10.056, PMID 29102700.
33. Song C, Repka MA. Hot-melt extrusion technology for transdermal patch development: a review. Drug Dev Ind Pharm. 2018;44(8):1080-93. doi: 10.1080/03639045.2018.1476834.
34. Di Nunzio JC, Leroux JC, Kasting GB. Hot-melt extrusion improves the properties of cyclodextrin-based poly(pseudo)rotaxanes for transdermal formulation. Int J Pharm. 2020;588:119724. doi: 10.1016/j.ijpharm.2019.119724.
35. Kochhar JS, Tan JJ, Kwang YC, Kang L. Introduction & literature review. In: Tan JJ, Kwang YC, Kang LC, editors. Microneedles for transdermal drug delivery. Berlin: Springer; 2019. p. 1-30. doi: 10.1007/978-3-030-15444-8_1.
36. Suwandecha T, Changklang P. Formulation development and characterization of a transdermal patch containing crinum asiaticum leaves extract. J Appl Pharm Sci. 2023;13(12):207-13. doi: 10.7324/JAPS.2023.151643.
37. Jaiswal P, Gidwani B, Vyas A. Nanostructured lipid carriers and their current application in targeted drug delivery. Artif Cells Nanomed Biotechnol. 2016;44(1):27-40. doi: 10.3109/21691401.2014.909822, PMID 24813223.
38. El-Houssiany A, Naguib Y, El-Amir A. Nanostructured lipid carriers for enhanced transdermal permeation of poorly soluble drugs. Colloids Surf B Biointerfaces. 2022;217:112598. doi: 10.1016/j.colsurfb.2022.112598.
39. Sriram N, Venkatesh R, Padmanabhan S. Novel backing membrane materials for improved transdermal patch stability. Drug Dev Ind Pharm. 2020;46(9):1510-8. doi: 10.1080/03639045.2020.1781467.
40. Gabriella Karger. Publishers note. Dig Dis. 2020;38(6):441. doi: 10.1159/000509675.
41. Jayaprakash R, Hameed J, Anupriya A. An overview of transdermal drug delivery system. Asian J Pharm Clin Res. 2017;10(10):36-40. doi: 10.22159/ajpcr.2017.v10i10.19909.
42. Kairanna NV, Singh BK, PP. Incidental detection of carcinoma in situ in fibroadenoma of breast in a young woman: a rare finding. Asian J Pharm Clin Res. 2019;12(1):1. doi: 10.22159/ajpcr.2018.v12i1.28326.
43. Ghanem AM. Recent advances in transdermal drug delivery systems of tamsulosin. Int J App Pharm. 2024;16(2):28-33. doi: 10.22159/ijap.2024v16i2.49950.
44. Prausnitz MR, Langer R. Transdermal drug delivery. Nat Biotechnol. 2008;26(11):1261-8. doi: 10.1038/nbt.1504, PMID 18997767.
45. Ita K. Transdermal delivery of drugs with microneedles: potential and challenges. Pharmaceutics. 2015;7(3):90-105. doi: 10.3390/pharmaceutics7030090, PMID 26131647.